

SCIENTIFIC REPORTS



OPEN

Single-photon multi-ports router based on the coupled cavity optomechanical system

Xun Li, Wen-Zhao Zhang, Biao Xiong & Ling Zhou

Received: 26 September 2016

Accepted: 18 November 2016

Published: 22 December 2016

A scheme of single-photon multi-port router is put forward by coupling two optomechanical cavities with waveguides. It is shown that the coupled two optomechanical cavities can exhibit photon blockade effect, which is generated from interference of three mode interaction. A single-photon travel along the system is calculated. The results show that the single photon can be controlled in the multi-port system because of the radiation pressure, which should be useful for constructing quantum network.

Quantum router to combine quantum channels with quantum nodes can create a quantum network so as to distribute quantum information. Recently, many theoretical proposals and experimental demonstrations of a quantum router have been carried out in various systems. One-dimensional single-photon efficient router in cavity QED system has been realized¹. By employing the EIT effect to guarantee single photon transportation, Io-Chun Hoi *et al.*² achieved a single-photon router in microwave regime. Different kinds of schemes of multi-port router have also been proposed, for instance cyclic three-level Δ -type atom system is used to route photon into two coupled cavity arrays^{3,4}. Linear-optical system^{5–8} also is regarded as a rational candidate of quantum router because of easy-control and easy-achieve property despite lack of capacity of routing single photon. Recently, people focus their vision on mesoscopic scale devices on account of its nonlinearity and controllability, such as optomechanical system⁹ and cavity electromechanical system¹⁰.

Photon-blockade phenomenon resulted from nonlinearity allows only one photon existence, and the second photon will be prohibited, which can be used to generate single photon source or to ensure a single photon processing. Cavity optomechanical systems, besides its potential application in detecting gravity waves^{11,12}, in studying quantum-to-classical transitions¹³, in performing high precision measurements^{14–17}, in entanglement generation^{18–20} and preservation²¹ and in processing quantum information^{16,22–25}, are of nonlinearity^{26–32}. But this nonlinear strength proportional to g^2/ω_m is limited by the condition g (the coupling strength of radiation pressure) less than ω_m (the frequency of the mechanical oscillator), therefore, a lot of effort is devoted to enhance the nonlinearity, for instance, adding atoms³³, introducing quantum dot³⁴, using coupled cavity optomechanical system²⁷ and employing three-mode mixing to generate effective photon blockade³⁵.

In this paper, we put forward a scheme by coupling two cavity optomechanical system. We show that our system can be effectively equal to three-mode interaction³⁵ and can exhibit photon blockade. Then we construct four output ports by coupling wave guide to the two-cavity-optomechanical system. Our research show that our system can work as multiple output ports router under the assistant of mechanical mode, which provide a potential application for the cavity optomechanical system in multiple router.

Results

In this part, we introduce our model, illustrate the photon-blockade effect of this two-cavity-optomechanical waveguide coupled system and study the transport of photons of waveguide under photon-blockade condition.

Model and effective interaction. We consider the two optomechanical cavities coupled with hopping coefficient J , and the two optomechanical cavities are side-coupled to the fibers respectively. The configuration of the system is shown in Fig. 1a, which is similar with ref. 36 where they utilized the two coupled whispering-gallery-mode (WGM) microtoroids coupled to two tapered fibers to experimentally realize parity-time-symmetric optics, but the mechanical modes are ignored. Taking the mechanical modes into consideration, we write the Hamiltonian as

School of Physics and Optoelectronic Technology, Dalian University of Technology, Dalian, 116024, People's Republic of China. Correspondence and requests for materials should be addressed to L.Z. (email: zhlihx@dlut.edu.cn)

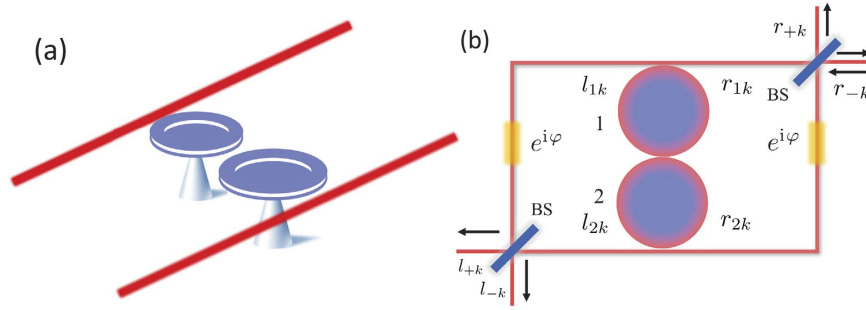


Figure 1. Schematic configuration of the single-photon router. (a) The two toroidal cavities with mechanical modes coupling to waveguide. (b) The four ports router with quasi-mode. The router consists of optomechanics as a single photon source, fibers, phase delayer with delay phase $\varphi = \frac{\pi}{2}$ and beam splitters to change photon from normal mode to quasi-mode.

$$\hat{H} = \hat{H}_{cav} + \hat{H}_{om} + \hat{H}_f \quad (1)$$

with

$$\begin{aligned} \hat{H}_{cav} &= \omega(\hat{a}_1^\dagger \hat{a}_1 + \hat{a}_2^\dagger \hat{a}_2) + J(\hat{a}_1^\dagger \hat{a}_2 + \hat{a}_1 \hat{a}_2^\dagger) + \sum_{j=1,2} \varepsilon_j (\hat{a}_j e^{i\omega_j t} + \hat{a}_j^\dagger e^{-i\omega_j t}), \\ \hat{H}_{om} &= \omega_m(\hat{b}_1^\dagger \hat{b}_1 + \hat{b}_2^\dagger \hat{b}_2) + g\hat{a}_1^\dagger \hat{a}_1(\hat{b}_1 + \hat{b}_1^\dagger) + g\hat{a}_2^\dagger \hat{a}_2(\hat{b}_2 + \hat{b}_2^\dagger), \end{aligned}$$

where \hat{H}_{cav} describes the free energy of the cavity, \hat{a}_1 (\hat{a}_2) and \hat{a}_1^\dagger (\hat{a}_2^\dagger) represent the annihilation and creation operators of cavity modes with the same frequency ω , and the two cavities are pumping with classical field with frequency ω_L and intensity $\varepsilon_1, \varepsilon_2$. \hat{H}_{om} represents the energy of the two mechanical oscillators with frequency ω_m and their coupling with the cavity fields induced by radiation pressure, where the \hat{b}_1 (\hat{b}_2) and \hat{b}_1^\dagger (\hat{b}_2^\dagger) are annihilation and creation operators of mechanical oscillators, g is coupling between first (second) cavity field and first (second) mechanical oscillator. The Hamiltonian \hat{H}_f in Eq. (1) can be written as

$$\hat{H}_f = \sum_{O=r,l} \sum_{j=1,2} \int_{-\infty}^{+\infty} dk [\omega_k \hat{O}_{jk}^\dagger \hat{O}_{jk} + i\xi(\hat{a}_j^\dagger \hat{O}_{jk} - \hat{a}_j \hat{O}_{jk}^\dagger)], \quad (2)$$

which expresses the two cavity fields coupling with the fibers, where \hat{O}_{jk} ($j = 1, 2; \hat{O} = r, l$) and ω_k represent annihilation operators and frequency of the fibers with wave number k , and ξ is the strength of coupling. In the frame rotating with $\hat{H}_0 = \omega_L[\hat{a}_1^\dagger \hat{a}_1 + \hat{a}_2^\dagger \hat{a}_2 + \sum_{\hat{O}=r,l} \int_{-\infty}^{+\infty} (\hat{O}_{1k}^\dagger \hat{O}_{1k} + \hat{O}_{2k}^\dagger \hat{O}_{2k}) dk]$, we have

$$\begin{aligned} \hat{H}'_{cav} &= \Delta(\hat{a}_1^\dagger \hat{a}_1 + \hat{a}_2^\dagger \hat{a}_2) - J(\hat{a}_1^\dagger \hat{a}_2 + \hat{a}_1 \hat{a}_2^\dagger) + \sum_{j=1,2} \varepsilon_j (\hat{a}_j + \hat{a}_j^\dagger), \\ \hat{H}'_{om} &= \omega_m(\hat{b}_1^\dagger \hat{b}_1 + \hat{b}_2^\dagger \hat{b}_2) + g\hat{a}_1^\dagger \hat{a}_1(\hat{b}_1 + \hat{b}_1^\dagger) + g\hat{a}_2^\dagger \hat{a}_2(\hat{b}_2 + \hat{b}_2^\dagger), \end{aligned} \quad (3)$$

where $\Delta = \omega - \omega_L$, and

$$\hat{H}_f = \sum_{O=r,l} \sum_{j=1,2} \int_{-\infty}^{+\infty} dk [\Delta_k \hat{O}_{jk}^\dagger \hat{O}_{jk} + i\xi(\hat{a}_j^\dagger \hat{O}_{jk} - \hat{a}_j \hat{O}_{jk}^\dagger)], \quad (4)$$

where $\Delta_k = \omega_k - \omega_L$. Now, we introduce the operators

$$\hat{a}_\pm = \frac{1}{\sqrt{2}}(\hat{a}_1 \pm \hat{a}_2), \quad \hat{b}_\pm = \frac{1}{\sqrt{2}}(\hat{b}_1 \pm \hat{b}_2),$$

The Hamiltonian $\hat{H}_s = \hat{H}_{cav} + \hat{H}_{om}$ is of the form

$$\begin{aligned} \hat{H}_s &= \Delta_+ \hat{a}_+^\dagger \hat{a}_+ + \Delta_- \hat{a}_-^\dagger \hat{a}_- + \varepsilon_- (\hat{a}_-^\dagger + \hat{a}_-) + \varepsilon_+ (\hat{a}_+^\dagger + \hat{a}_+) + \omega_m \hat{b}_+^\dagger \hat{b}_+ + \omega_m \hat{b}_-^\dagger \hat{b}_- \\ &+ \frac{g}{\sqrt{2}}(\hat{b}_+ + \hat{b}_+^\dagger)(\hat{a}_+^\dagger \hat{a}_+ + \hat{a}_+ \hat{a}_+^\dagger) + \frac{g}{\sqrt{2}}(\hat{b}_- + \hat{b}_-^\dagger)(\hat{a}_-^\dagger \hat{a}_- + \hat{a}_- \hat{a}_-^\dagger), \end{aligned} \quad (5)$$

where $\Delta_\pm = \Delta \mp J$, $\varepsilon_\pm = \frac{\varepsilon_1 \pm \varepsilon_2}{\sqrt{2}}$. For the fiber, we define

$$\hat{r}_{\pm k} = \frac{1}{\sqrt{2}}(\hat{r}_{1k} \pm \hat{r}_{2k}), \quad \hat{l}_{\pm k} = \frac{1}{\sqrt{2}}(\hat{l}_{1k} \pm \hat{l}_{2k}), \quad \hat{a}_{\pm k} = \frac{\hat{r}_{\pm k} + \hat{l}_{\pm k}}{\sqrt{2}}, \quad \hat{c}_{\pm k} = \frac{\hat{r}_{\pm k} - \hat{l}_{\pm k}}{\sqrt{2}}. \quad (6)$$

Thus, \hat{H}_f can be rewritten as

$$\hat{H}_f = \int_0^\infty \Delta_k dk \left[\hat{a}_{+k}^\dagger \hat{a}_{+k} + \hat{a}_{-k}^\dagger \hat{a}_{-k} + \hat{c}_{+k}^\dagger \hat{c}_{+k} + \hat{c}_{-k}^\dagger \hat{c}_{-k} \right] + \sqrt{2} \xi \int_0^\infty dk [\hat{a}_+^\dagger \hat{a}_{+k} + \hat{a}_-^\dagger \hat{a}_{-k} + h. c.]. \quad (7)$$

We see that the cavity modes are decoupled with the fiber mode \hat{c}_{+k} and \hat{c}_{-k} . We switch into the picture rotating with $\hat{U} = \exp\{-it[-2J(\hat{a}_+^\dagger \hat{a}_+ + \int_0^\infty \Delta_k dk \hat{a}_{+k}^\dagger \hat{a}_{+k}) + \omega_m(\hat{b}_+^\dagger \hat{b}_+ + \hat{b}_-^\dagger \hat{b}_-)]\}$, i.e., employing the relation $\hat{H}_i = \hat{U}^\dagger \hat{H}_i \hat{U} - iU^\dagger \dot{U}$, we can rewrite Eq. (5). Considering the condition $\{\omega_m, J\} \gg \{g, \varepsilon_+\}$ and choosing parameters $\omega_m = 2J$, we have the Hamiltonian

$$\hat{H}_{si} = \Delta_-(\hat{a}_+^\dagger \hat{a}_+ + \hat{a}_-^\dagger \hat{a}_-) + \varepsilon_-(\hat{a}_+^\dagger + \hat{a}_-) + \frac{g}{\sqrt{2}}(\hat{a}_+^\dagger \hat{a}_- \hat{b}_+^\dagger + \hat{a}_+ \hat{a}_-^\dagger \hat{b}_-), \quad (8)$$

and

$$\hat{H}_{fi} = \int_0^\infty dk [\Delta_{kj} \hat{a}_{+k}^\dagger \hat{a}_{+k} + \Delta_k (\hat{a}_{-k}^\dagger \hat{a}_{-k} + \hat{c}_{+k}^\dagger \hat{c}_{+k} + \hat{c}_{-k}^\dagger \hat{c}_{-k})] + \sqrt{2} \xi \int_0^\infty dk [\hat{a}_+^\dagger \hat{a}_{+k} + \hat{a}_-^\dagger \hat{a}_{-k} + h. c.]. \quad (9)$$

where $\Delta_{kj} = \Delta_k + 2J$. Due to rotating-wave approximation, the terms $\varepsilon_+(\hat{a}_+^\dagger e^{-2ijt} + \hat{a}_+ e^{2ijt})$, $\frac{g}{\sqrt{2}}(\hat{b}_+ e^{-i\omega_m t} + \hat{b}_+^\dagger e^{i\omega_m t})(\hat{a}_+^\dagger \hat{a}_+ + \hat{a}_-^\dagger \hat{a}_-)$ and $\frac{g}{\sqrt{2}}(\hat{b}_- \hat{a}_+^\dagger e^{-i(\omega_m+2J)t} + \hat{b}_-^\dagger e^{i(\omega_m+2J)t})$ with high frequency oscillation are ignored. The Hamiltonian Eq. (8) indicate the three-body interaction between cavities and the oscillator, which is exact the same with ref. 35 where the nonlinearity has been analyzed. In a single cavity optomechanical system, the effective photon-photon interactions g^2/ω_m is suppressed by the condition that the mechanical frequency is much larger than the coupling g , i.e., $\omega_m \gg g$, while the three-body interaction (8) has its advantage³⁵ that photons in the two optical modes can be resonantly exchanged by absorbing or emitting a phonon via three-mode mixing; therefore, the restraint $\omega_m \gg g$ can be overcome. Since our system can be simplified as³⁵, one can see that the nonlinearity should exist and does not restrict by the condition $\omega_m \gg g$. Most importantly, the Hamiltonian Eqs (8) and (9) exhibit clearly the conversion between the quasi-mode between \hat{a}_+ and \hat{a}_- under the witness of \hat{b}_- so that we can realize the exchange between \hat{a}_{+k} and \hat{a}_{-k} . Therefore, with the interaction, we can potentially realize four ports router.

Photon Blockade. Now we first investigate the nonlinearity of the photons within the cavity. The dynamics of the system obeys the master equation

$$\frac{d\hat{\rho}}{dt} = -i[\hat{H}'_{cav} + \hat{H}'_{om}, \hat{\rho}] + \sum_{i=1,2} (\hat{L}_{\hat{a}_i} + \hat{D}_{\hat{b}_i})\hat{\rho} \quad (10)$$

where Lindblad $\hat{L}_{\hat{a}_i} = \kappa(2\hat{a}_i \cdot \hat{a}_i^\dagger - \hat{a}_i^\dagger \hat{a}_i \cdot - \cdot \hat{a}_i^\dagger \hat{a}_i)$ with zero thermal photon and dissipation rate κ , $\hat{D}_{\hat{b}_i} = \gamma_m(n_{thm} + 1)(2\hat{b}_i \cdot \hat{b}_i^\dagger - \hat{b}_i^\dagger \hat{b}_i \cdot - \cdot \hat{b}_i^\dagger \hat{b}_i) + \gamma_m n_{thm}(2\hat{b}_i \cdot \hat{b}_i - \hat{b}_i \hat{b}_i^\dagger \cdot - \cdot \hat{b}_i \hat{b}_i^\dagger)$ with thermal photon n_{thm} and dissipation rate γ_m , $i = 1, 2$. The fibers can be considered as a part of environment of the cavity modes with the interaction (4), thus, the interaction between the cavities and the fibers can be reduced to the term $\hat{L}_{\hat{a}_i}$. Similarly, the interaction (9) also can be reduced into Lindblad form. Because of the larger frequency difference ($\omega \gg \omega_m$), the cavity fields can be treated as in environment with zero thermal photon while for the mechanical oscillators they are involved in thermal reservoir. To characterize the nonlinearity of optical modes, we employ the equal-time second-order correlation functions

$$g_{ij}^{(2)}(0) = \frac{\langle \hat{a}_i^\dagger \hat{a}_j^\dagger \hat{a}_j \hat{a}_i \rangle}{\langle \hat{a}_i^\dagger \hat{a}_i \rangle \langle \hat{a}_j^\dagger \hat{a}_j \rangle}. \quad (11)$$

For $i = j$, the function $g_{ii}^{(2)}(0) [g_{ij}^{(2)}(0)]$ denotes the self-correlation, and $g_{ij}^{(2)}(0)$ ($i \neq j$) express the cross-correlation. If the correlation function $g_{ij}^{(2)}(0) < 1$ we say the photon anti-bunching, and the limit $g_i^{(2)}(0) = 0$ corresponds to the thorough photon blockade effect, which means that only one photon can exist, and the another photon will be blocked.

Now, we show the nonlinearity by comparing the numerically solution of the master equation Eq. (10) with that $\hat{H}'_{cav} + \hat{H}'_{om}$ are substituted with effective Hamiltonian Eq. (8) where the subscripts $i = 1, 2$ for the superoperators $\hat{L}_{\hat{a}_i}$ and $\hat{D}_{\hat{b}_i}$ are easily changed to $i = -, +$ because we assume the two cavity modes as well as mechanical modes with equal decay rate respectively. As shown in Fig. 2, we see that the solution of master equation with the effective Hamiltonian coincides with that of master equation with original Hamiltonian, which show that the effective Hamiltonian method is reliable. We will employ the effective Hamiltonian Eq. (8) in the calculation of the photon router procession. More importantly, we observe that $g_{ij}^{(2)}(0)$ ($i, j = -, +$) achieves their minimum values around $\Delta_- = \pm \frac{g}{\sqrt{2}}$, which means that the system can suppress the simultaneous two-photon creations in

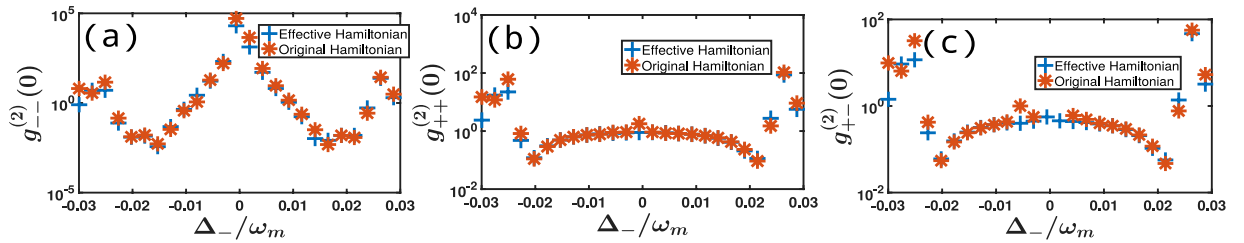


Figure 2. (a) Plot a relation between correlation function $g_{--}^{(2)}(0)$ and detuning Δ_- , blue dot for solve master equation with effective Hamiltonian red dot for original Hamiltonian. (b) Correction $g_{++}^{(2)}(0)$ of a_+ as function of Δ_- . (c) Cross correlation function $g_{+-}^{(2)}(0)$ versus detuning Δ_- . Other parameters are $J=2\omega_m, g=0.03\omega_m, \kappa=10^{-3}\omega_m, n_{mth}=0.2, \gamma_m=\kappa/200, \varepsilon_1=1.1 \times 10^{-4}\omega_m, \varepsilon_2=-\varepsilon_1$.

any of the mode \hat{a}_- and \hat{a}_+ , especially the cross mode between \hat{a}_- and \hat{a}_+ . That is to say, in the coupled two cavity optomechanical system, there is most possible only one photon existence. Thus, the property can be potentially used as a single photon router if we can control it. The photon-blockade is resulted from three-body interactions that lead to destructive interference of optical modes. The conclusion is also obtained in ref. 35 where the destructive interference is analyzed with eigenstate of the Hamiltonian Eq. (8). The three-body interaction is still dependent on the coupling g see Eq. (8), therefore the strong coupling strength is still welcome. But the nonlinearity is not proportional to $\frac{g^2}{\omega_m}$, which means that the nonlinearity is not limited by the condition $g \ll \omega_m$.

Single-photon router. Quantum router is a hinge device for large-scale network communications. How to design quantum router arouse a lot of interests^{1-5,9,10}. To satisfy the requirements of quantum information, a single-photon quantum router will be demanded. Photon blockade effect is an effective method to realize the single-photon router. As we have shown in the Fig. 2, there is a good photon blockade phenomenon in this optomechanical system. We can reasonably assume that the device is only allow a single photon transport. Therefore we will only consider a single excitation in the system.

Now, we employ the two coupled optomechanical cavities to couple to two waveguide (CRW) shown in Fig. 1b. In order to employ the quasi-mode, we introduce medium as phase shifter and beam splitters to generate the quasi-mode. One can easy deduce that the four outputs will satisfy the relation Eq. (6). We now calculate the photon number of the four ports. Under the Hamiltonian Eqs (8) and (9), the basis is denoted as $|n_-, n_+, n_b, n_{d-k}, n_{d+k}\rangle$, thus we can write the wave function with only a single excitation as

$$|\Psi(t)\rangle = \alpha_-|1, 0, 0, 0, 0\rangle + \alpha_+|0, 1, 1, 0, 0\rangle + \int_0^\infty dk [\mu_k|0,0,0,1_k, 0\rangle + \eta_k|0, 0, 1, 0, 1_k\rangle], \quad (12)$$

In terms of the left- and right-propagation modes, if we assume a photon packet is incident onto the cavity from the port \hat{r}_{-k} , i.e., $|\Psi(0)\rangle = \int_0^\infty dk \mu_k(0) \hat{r}_{-k} |\emptyset\rangle$, a wave packet with a Lorentzian spectrum $\mu_k(0) = \frac{G_1}{\Delta_k - \delta + i\varepsilon}$, where ε and G_1 are the linewidth and normalization coefficient of Lorentzian spectrum. The wave function obey Schrodinger equation with Hamiltonian $\hat{H} = \hat{H}_s + \hat{H}_f$. In the long-time limit, we can find the solution of wave function

$$|\Psi(t \rightarrow \infty)\rangle = \int_0^\infty dk [\mu_k(0) e^{-i\Delta_k t} (r_{-k} \hat{r}_{-k} + L_{-k} \hat{l}_{-k}) + \mu_k'(0) e^{-i\Delta_k t} (r_{+k} \hat{r}_{+k} + L_{+k} \hat{l}_{+k})] |\emptyset\rangle.$$

The details of calculation can be found in part methods. Therefore, the output photon number of the four ports are obtained as

$$N_{r_-}^{(out)} = \frac{\pi |G_1|^2}{\varepsilon} - 2\pi |G_1|^2 \gamma^2 \left[\frac{1}{\varepsilon} \frac{\gamma^2 + g^2 + (\delta' + \varepsilon)^2}{\mathcal{F}_{++}\mathcal{F}_{+-}\mathcal{F}_{-+}\mathcal{F}_{--}} + \frac{\sqrt{2}}{4g\gamma} \left(\frac{1}{g/\sqrt{2} + i\gamma} \frac{3g^2/2 - i\sqrt{2}g\gamma}{\mathcal{F}_{++}^* \mathcal{F}_{+-}} + \frac{1}{g/\sqrt{2} - i\gamma} \frac{3g^2/2 + i\sqrt{2}g\gamma}{\mathcal{F}_{-+}^* \mathcal{F}_{--}} \right) \right] \quad (13)$$

$$N_{l_-}^{(out)} = 2\pi |G_1|^2 \gamma^2 \left[\frac{1}{\varepsilon} \frac{\gamma^2 + (\delta' + \varepsilon)^2}{\mathcal{F}_{++}\mathcal{F}_{+-}\mathcal{F}_{-+}\mathcal{F}_{--}} + \frac{\sqrt{2}}{4g\gamma} \left(\frac{1}{g/\sqrt{2} + i\gamma} \frac{g^2/2 - i\sqrt{2}g\gamma}{\mathcal{F}_{++}^* \mathcal{F}_{+-}} + \frac{1}{g/\sqrt{2} - i\gamma} \frac{g^2/2 + i\sqrt{2}g\gamma}{\mathcal{F}_{-+}^* \mathcal{F}_{--}} \right) \right] \quad (14)$$

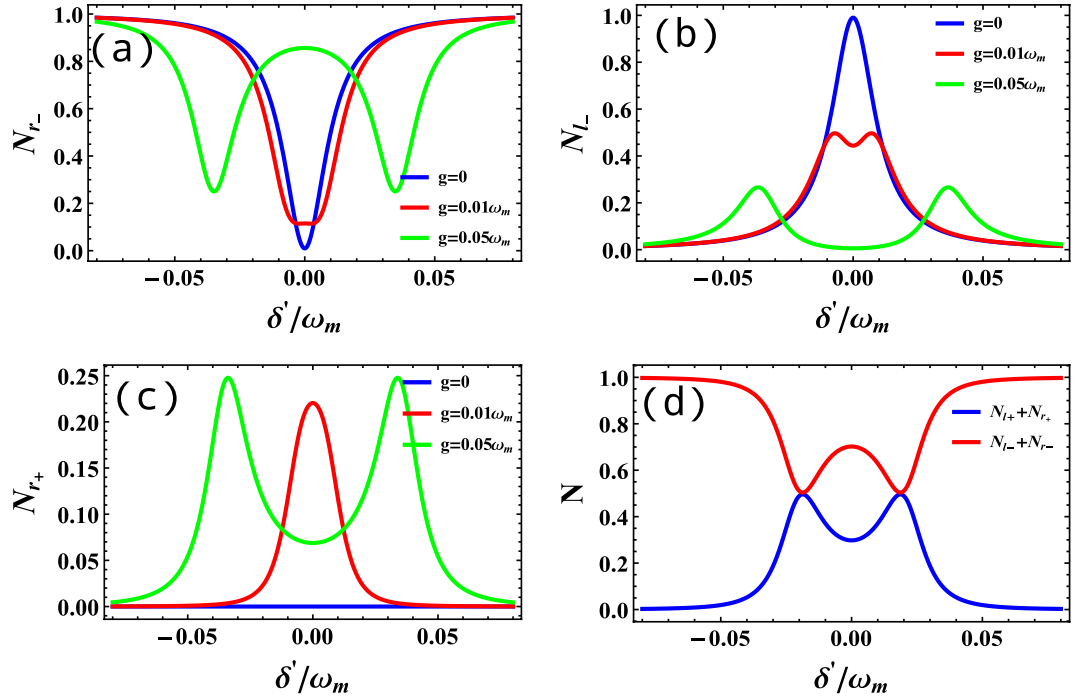


Figure 3. (a–c) Photon number N_{r-} , N_{l-} , N_{r+} as function of δ' for several values of g where $\gamma = 0.01\omega_m$. (d) $N_{l+} + N_{r+}$ and $N_{l-} + N_{r-}$ as function of δ' with $g = 0.04\omega_m$. It is naturally satisfied normalized condition $N_{l+} + N_{r+} + N_{l-} + N_{r-} = 1$. And $\varepsilon = 0.0001\omega_m$ all the parameters were normalized by ω_m .

$$N_{r+}^{(out)} = \pi |G_1|^2 g^2 \gamma^2 \left[\frac{1}{\varepsilon \mathcal{F}_{++} \mathcal{F}_{+-} \mathcal{F}_{-+} \mathcal{F}_{--}} + \frac{\sqrt{2}}{4g\gamma} \left(\frac{1}{g/\sqrt{2} + i\gamma \mathcal{F}_{++}^* \mathcal{F}_{+-}} + \frac{1}{g/\sqrt{2} - i\gamma \mathcal{F}_{-+}^* \mathcal{F}_{--}} \right) \right] \quad (15)$$

$$N_{l+}^{(out)} = N_{r+}^{(out)} \quad (16)$$

with $\mathcal{F}_{\pm\pm} = \delta' \pm g/\sqrt{2} \pm \gamma + i\varepsilon$, where $\delta' = \delta - \Delta_-$ and $\gamma = 2\pi\xi^2$. The detail can be seen in the section of method. We can clearly see that if $g = 0$, $N_{l+}^{(out)} = N_{r+}^{(out)} = 0$, and $N_{r-}^{(out)}(N_{l-}^{(out)}) \neq 0$, which means that without the mechanical oscillator we only have two-port router, and the optomechanical coupling is necessary for us to realize multi-port router.

We plot the output photon number of the four ports as a function of δ' for several values of g in Fig. 3(a–c). If $g = 0$ (means without the coupling of radiation pressure), when $\delta' = 0$ ($\delta = \Delta_-$ denotes that the input photon is on resonant with the cavity fields), the single photon will almost transmit into the left port \hat{l}_- which was equivalent to a common cavity waveguide coupled system which present a perfect reflection at resonance region and only one peaks (valleys) with linewidth 2γ showing in blue line of Fig. 3(a,b). With the increasing of g , the photon will be partially transmitted and partially be reflected, but they are still of one peak (valley). However, with the increasing the values of g , for example $g = 0.05\omega_m$, the single peak (valley) is split into two peaks (valleys) because the movable mirror participates the three-body interaction so that we can see the symmetry peaks (valleys). Most importantly, the one port input signal can be distributed into four ports see Fig. 3(a–c), while for $g = 0$, we can receive only two ports signals N_{l-} and N_{r-} . Therefore, with the assistant of the two coupled cavity optomechanical system, we can realize multi-port router. We parcel the four-port output into two parts $N_{l+} + N_{r+}$, $N_{l-} + N_{r-}$ because they denote the difference whether the optomechanical coupling is included or not, seeing Fig. 3(d). Though we can transport the photon via the optomechanical coupling, the probability of transportation $N_{l+} + N_{r+}$ is still less than $N_{l-} + N_{r-}$ under the group of the parameters, which means that the optomechanical coupling constant g strong affects the router process.

Besides the optomechanical interaction, the cavity-fiber coupling should also have important influence on the router process. As shown in Fig. 4(a–c), we plot the multi-port output photon number under the same optomechanical coupling $g = 0.02\omega_m$ but with different cavity-fiber coupling constants γ . For $\gamma = 0.05\omega_m$, we can observe the split of peaks (valleys). However, with the increasing of γ , even with the same optomechanical interaction g , one only can see single peak (valley), which means that strong cavity-fiber coupling can suppress the function of optomechanical coupling. That is to say, there is a competitive relation between and cavity-fiber interaction and

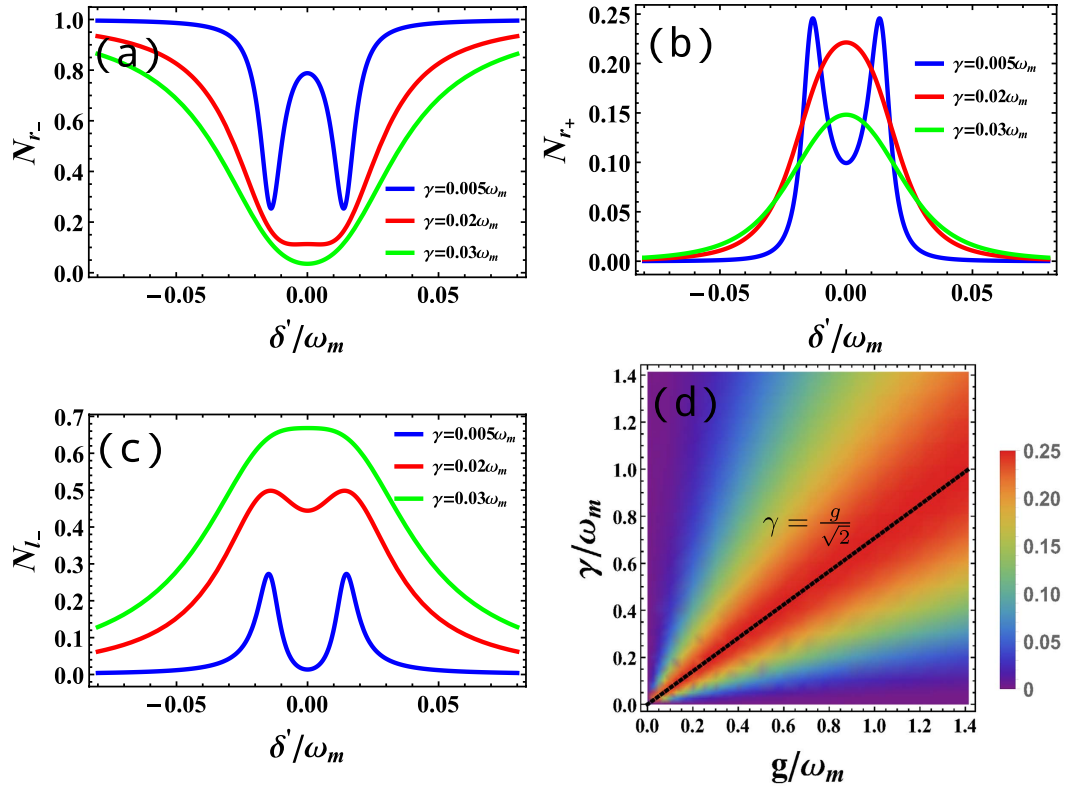


Figure 4. (a–c) Photon number N_{r-} , N_{l-} , N_{r+} as function of δ' for several values of $\gamma = 0.005\omega_m$, $0.02\omega_m$, $0.03\omega_m$ represented by blue, red, green line respectively, where $g = 0.02\omega_m$. (d) Photon number N_{l+} (N_{r+}) versus γ and g when $\delta' = 0$. The dash black line highlight the maximum of output. G_1 is a normalization coefficient to guarantee $N_{l+} + N_{r+} + N_{l-} + N_{r-} = 1$, $\varepsilon = 0.0001\omega_m$ all the parameters were normalized by ω_m .

the optomechanical coupling. In order to make clear the match relation, we plot optimized N_{r+} (N_{l+}) as function of the parameters g and γ , shown in Fig. 4(d). We observe that when there is an optimized value N_{r+} (N_{l+}) along the line $\gamma = \frac{g}{\sqrt{2}}$, which exhibit that the balance between cavity waveguide coupling and optomechanical interaction is helpful to the multi-port router procession.

Conclusion

We put forward a scheme to realize multi-port router using two coupled cavity optomechanical system. We first demonstrate that our system with the Hamiltonian Eq. (8) can be effectively equal to the three-body interaction between cavities and the oscillator which has been shown in ref. 35. The nonlinearity in the three-mode mixing is not proportion to g^2/ω_m and can overcome the restraint $\omega_m \gg g$. We also numerically show the nonlinearity and correction of the effective interaction. By coupling the two coupled cavity optomechanical system to waveguide, we calculate the output photon number of the multi-port router. Our results show that the presented system can work as multi-port router under the witness of the optomechanical coupling. Since the two coupled optomechanical cavity is similar with the experiment³⁶ where the optomechanical coupling is ignored. If the optomechanical coupling is strong enough, our scheme should be realizable.

Methods

Router. Now we solve the Schrodinger equation of this system with Hamiltonian $\hat{H} = \hat{H}_s + \hat{H}_f$ and wave function Eq. (12).

$$\begin{aligned}
 \dot{\alpha}_- &= -i \left[\Delta_- \alpha_- + \frac{g}{\sqrt{2}} \alpha_+ + \sqrt{2} \xi \int_0^\infty dk \mu_k \right], \\
 \dot{\alpha}_+ &= -i \left[\Delta_- \alpha_+ + \frac{g}{\sqrt{2}} \alpha_- + \sqrt{2} \xi \int_0^\infty dk \eta_k \right], \\
 \dot{\mu}_k &= -i [\Delta_k \mu_k + \sqrt{2} \xi \alpha_-], \\
 \dot{\eta}_k &= -i [\Delta_{kj} \eta_k + \sqrt{2} \xi \alpha_+].
 \end{aligned}
 \tag{17}$$

We assume that initially the cavity is in the vacuum state, and a single photon with the waveguide, i.e., $|0, 0, 0, 1_k, 0\rangle$ is prepared in a wave packet with a Lorentzian spectrum, the initial condition reads $\mu_k(0) = \frac{G_1}{\Delta_k - \delta + i\varepsilon}$. Using Laplace transformation, the differential equations Eq. (17) become

$$\begin{aligned} s\tilde{\alpha}_- &= -i\left[\Delta_- \tilde{\alpha}_- + \frac{g}{\sqrt{2}} \tilde{\alpha}_+ + \sqrt{2}\xi \int_0^\infty dk \tilde{\mu}_k\right], \\ s\tilde{\alpha}_+ &= -i\left[\Delta_- \tilde{\alpha}_+ + \frac{g}{\sqrt{2}} \tilde{\alpha}_- + \sqrt{2}\xi \int_0^\infty dk \tilde{\eta}_k\right], \\ s\tilde{\mu}_k &= -i[\Delta_k \tilde{\mu}_k + \sqrt{2}\xi \tilde{\alpha}_-] + \mu_k(0), \\ s\tilde{\eta}_k &= -i[\Delta_{kj} \tilde{\eta}_k + \sqrt{2}\xi \tilde{\alpha}_+], \end{aligned} \quad (18)$$

In the long-time limit, the coefficients $\mu_k(\infty)$ and $\eta_k(\infty)$ are obtained after inverse Laplace transformation as

$$\begin{aligned} \mu_k(\infty) &= \frac{2(\gamma^2 + \tilde{\Delta}_k^2) - g^2}{2(\tilde{\Delta}_k + i\gamma)^2 - g^2} \mu_k(0) e^{-i\Delta_k t}, \\ \eta_k(\infty) &= -\frac{2\sqrt{2}ig\gamma}{2(\tilde{\Delta}_{kj} + i\gamma)^2 - g^2} \mu_k'(0) e^{-i\Delta_{kj} t}. \end{aligned} \quad (19)$$

where $\gamma = 2\pi\xi^2$ denoting the cavities loss into the waveguide. If there is no the other decay except the exchange between the cavities and the waveguide, γ will be equal to the decay rate of the cavity which we have mentioned in Fig. 2. In terms of the left- and right-propagation modes, if we assume a photon packet is incident onto the cavity from the port r_{-k} , then the initial state can be written as

$$|\Psi(0)\rangle = \int_0^\infty dk \mu_k(0) \hat{r}_{-k} |\emptyset\rangle = \frac{1}{\sqrt{2}} \int_0^\infty dk \mu_k(0) (\hat{d}_{-k} + \hat{c}_{-k}) |\emptyset\rangle, \quad (20)$$

which means that the single photon input from the port r_{-k} can be considered as a superposition between a quasiparticle \hat{d}_{-k} and a quasiparticle \hat{c}_{-k} . In the long-time limit, the wave function becomes under the Hamiltonian Eqs (8) and (9)

$$|\Psi(t \rightarrow \infty)\rangle = \int_0^\infty dk [\mu_k(0) e^{-i\Delta_k t} (r_{-k} \hat{r}_{-k} + l_{-k} \hat{l}_{-k}) + \mu_k'(0) e^{-i\Delta_{kj} t} (r_{+k} \hat{r}_{+k} + l_{+k} \hat{l}_{+k})] |\emptyset\rangle$$

where the first bracket with the factor $e^{-i\Delta_k t}$ can survive without Hamiltonian Eq. (8), while the second bracket with the factor $e^{-i\Delta_{kj} t}$ survive only under the condition Eq. (8) existence. In other words, the photon on the ports r_{-k} and l_{-k} can be detected even without the mechanical mode, however, if we would like to obtain photon on the port r_{+k} and l_{+k} , the coupling between the mechanical mode and cavity field is necessary. Then we obtain

$$\begin{aligned} r_{-k} &= \sqrt{2} \frac{(\gamma^2 + \tilde{\Delta}_k^2) + (\tilde{\Delta}_k + i\gamma)^2 - g^2}{2(\tilde{\Delta}_k + i\gamma)^2 - g^2}, \\ l_{-k} &= \sqrt{2} \frac{\gamma^2 + \tilde{\Delta}_k^2 - (\tilde{\Delta}_k + i\gamma)^2}{2(\tilde{\Delta}_k + i\gamma)^2 - g^2}, \\ l_{+k} &= -\frac{2ig\gamma}{2(\Delta_k + i\gamma)^2 - g^2}, \\ r_{+k} &= l_{+k}, \end{aligned} \quad (21)$$

and the output photon number in Eqs (14), (15) and (16).

References

- Aoki, T., Parkins, A., Alton, D., Regal, C., Dayan, B., Ostby, E., Vahala, K. & Kimble, H. Efficient Routing of Single Photons by One Atom and a Microtoroidal Cavity. *Phys. Rev. Lett.* **102**, 083601 (2009).
- Hoi, I. C., Wilson, C. M., Johansson, G., Palomaki, T., Peropadre, B. & Delsing, P. Demonstration of a single-photon router in the microwave regime. *Phys. Rev. Lett.* **107**, 073601 (2011).
- Zhou, L., Yang, L. P., Li, Y. & Sun, C. P. Quantum routing of single photons with a cyclic three-level system. *Phys. Rev. Lett.* **111**, 103604 (2013).
- Lu, J., Zhou, L., Kuang, L. M. & Nori, F. Single-photon router: Coherent control of multichannel scattering for single photons with quantum interferences. *Phys. Rev. A* **89**, 013805 (2014).
- Lemr, K., Bartkiewicz, K., Černoč, A. & Soubusta, J. Resource-efficient linear-optical quantum router. *Phys. Rev. A* **87**, 062333 (2013).
- Yan, W.-B., Liu, B., Zhou, L. & Fan, H. All-optical router at single-photon level by interference. *EPL (Europhysics Lett.)* **111**, 64005 (2015).
- Chen, X.-Y., Zhang, F.-Y. & Li, C. Single-photon quantum router by two distant artificial atoms. *J. Opt. Soc. Am. B* **33**, 583–588 (2016).
- Yuan, X. X., Ma, J. J., Hou, P. Y., Chang, X. Y., Zu, C. & Duan, L. M. Experimental demonstration of a quantum router. *Sci. Rep.* **5**, 12452 (2015).
- Agarwal, G. S. & Huang, S. Optomechanical systems as single-photon routers. *Phys. Rev. A* **85**, 021801 (2012).

10. Jiang, C., Chen, B. & Zhu, K.-D. Demonstration of a single-photon router with a cavity electromechanical system. *J. Appl. Phys.* **112**, 033113 (2012).
11. Ma, Y., Danilishin, Shtenfan L., Zhao, Chunnnong, Miao, Haixing, Korth, W. Z., Chen, Yanbei, Ward, Robert L. & Blair, D. G. Narrowing the Filter-Cavity Bandwidth in Gravitational-Wave Detectors via Optomechanical Interaction. *Phys. Rev. Lett.* **113**, 151102 (2014).
12. LIGO Scientific Collaboration. Observation of a kilogram-scale oscillator near its quantum ground state. *New J. Phys.* **11**, 073032 (2009).
13. Ghobadi, R., Kumar, S., Pepper, B., Bouwmeester, D., Lvovsky, a. I. & Simon, C. Optomechanical Micro-Macro Entanglement. *Phys. Rev. Lett.* **112**, 080503 (2014).
14. Zhang, K., Bariani, F., Dong, Y., Zhang, W. & Meystre, P. Proposal for an Optomechanical Microwave Sensor at the Subphoton Level. *Phys. Rev. Lett.* **114**, 1–6 (2015).
15. Barzanjeh, S., Guha, Saikat, Weedbrook, Christian, Vitali, David, Shapiro, Jeffrey H. & Pirandola, Stefano Microwave quantum illumination. *Phys. Rev. Lett.* **114**, 1–5 (2015).
16. Kippenberg, T. J., Schliesser, A. & Gorodetsky, M. L. Phase noise measurement of external cavity diode lasers and implications for optomechanical sideband cooling of ghz mechanical modes. *New Journal of Physics* **15**, 015019 (2013).
17. Chen, Y. Macroscopic quantum mechanics: theory and experimental concepts of optomechanics. *J. Phys. B At. Mol. Opt. Phys.* **46**, 104001 (2013).
18. Vitali, D. *et al.* Optomechanical entanglement between a movable mirror and a cavity field. *Phys. Rev. Lett.* **98**, 1–4 (2007).
19. Bai, C.-H., Wang, D.-Y., Wang, H.-F., Zhu, A.-D. & Zhang, S. Robust entanglement between a movable mirror and atomic ensemble and entanglement transfer in coupled optomechanical system. *Sci. Rep.* 33404 (2016).
20. Mu, Q., Zhao, X. & Yu, T. Memory effect induced macroscopic-microscopic entanglement. *Phys. Rev. A* **94**, 012334 (2016).
21. Cheng, J., Zhang, W.-Z., Zhou, L. & Zhang, W. Preservation Macroscopic Entanglement of Optomechanical Systems in non-Markovian Environment. *Sci. Rep.* **6**, 23678 (2016).
22. Zhang, W.-Z., Cheng, J., Liu, J.-Y. & Zhou, L. Controlling photon transport in the single-photon weak-coupling regime of cavity optomechanics. *Phys. Rev. A* **91**, 063836 (2015).
23. Li, W., Jiang, Y., Li, C. & Song, H. Parity-time-symmetry enhanced optomechanically-induced-transparency. *Sci. Rep.* **6**, 31095 (2016).
24. Dalafi, A., Naderi, M. H., Soltanolkotabi, M. & Barzanjeh, S. Controllability of optical bistability, cooling and entanglement in hybrid cavity optomechanical systems by nonlinear atom-atom interaction. *J. Phys. B At. Mol. Opt. Phys.* **46**, 235502 (2013).
25. Xu, X.-W. & Li, Y. Controllable optical output fields from an optomechanical system with mechanical driving. *Phys. Rev. A* **92**, 023855 (2015).
26. Gong, Z. R., Ian, H., Liu, Y. X., Sun, C. P. & Nori, F. Effective hamiltonian approach to the Kerr nonlinearity in an optomechanical system. *Phys. Rev. A* **80**, 065801 (2009).
27. Ludwig, M., Safavi-Naeini, A. H., Painter, O. & Marquardt, F. Enhanced Quantum Nonlinearities in a Two-Mode Optomechanical System. *Phys. Rev. Lett.* **109**, 063601 (2012).
28. Liao, J.-q., Law, C. K., Kuang, L.-m. & Nori, F. Enhancement of mechanical effects of single photons in modulated two-mode optomechanics. *Phys. Rev. A* **92**, 013822 (2015).
29. Liu, Y.-L., Liu, Z.-P. & Zhang, J. Coherent-feedback-induced controllable optical bistability and photon blockade. *J. Phys. B At. Mol. Opt. Phys.* **48**, 105501 (2015).
30. Flayac, H., Gerace, D. & Savona, V. An all-silicon single-photon source by unconventional photon blockade. *Sci. Rep.* **5**, 11223 (2015).
31. Rabl, P. Photon blockade effect in optomechanical systems. *Phys. Rev. Lett.* **107**, 063601 (2011).
32. Wang, H., Gu, X., Liu, Y.-x., Miranowicz, A. & Nori, F. Tunable photon blockade in a hybrid system consisting of an optomechanical device coupled to a two-level system. *Phys. Rev. A* **92**, 033806 (2015).
33. Zhou, L., Han, Y., Jing, J. & Zhang, W. Entanglement of nanomechanical oscillators and two-mode fields induced by atomic coherence. *Phys. Rev. A* **83**, 052117 (2011).
34. Tang, J., Geng, W. & Xu, X. Quantum interference induced photon blockade in a coupled single quantum dot-cavity system. *Sci. Rep.* **5**, 9252 (2015).
35. Kómar, P., Bennett, S., Stannigel, K., Habraken, S., Rabl, P., Zoller, P. & Lukin, M. Single-photon nonlinearities in two-mode optomechanics. *Phys. Rev. A* **87**, 013839 (2013).
36. Chang, L., Jiang, Xiaoshun, Hua, Shiyue, Yang, Chao, Wen, Jiangming, Jiang, Liang, Li, Guanyu, Wang, Guanzhong & Xiao, Min. Parity-time symmetry and variable optical isolation in active-passive-coupled microresonators. *Nature Photonics* **8**, 524–529 (2014).

Acknowledgements

We would like to thank Wei-bin Yan for helpful discussions. This work was supported by the NSF of China under Grant No. 11474044.

Author Contributions

X.L. and L.Z. designed the research, X.L. did the analytic calculations, W.Z.Z. provided help in numerical calculation and prepared figures, B.X. had an important contribution to modify manuscript, L.Z. revised the manuscript and provided overall theoretical support.

Additional Information

Competing financial interests: The authors declare no competing financial interests.

How to cite this article: Li, X. *et al.* Single-photon multi-ports router based on the coupled cavity optomechanical system. *Sci. Rep.* **6**, 39343; doi: 10.1038/srep39343 (2016).

Publisher's note: Springer Nature remains neutral with regard to jurisdictional claims in published maps and institutional affiliations.



This work is licensed under a Creative Commons Attribution 4.0 International License. The images or other third party material in this article are included in the article's Creative Commons license, unless indicated otherwise in the credit line; if the material is not included under the Creative Commons license, users will need to obtain permission from the license holder to reproduce the material. To view a copy of this license, visit <http://creativecommons.org/licenses/by/4.0/>

© The Author(s) 2016